Graphitic carbon nitride (g-C$_3$N$_4$) can be fabricated in minutes by microwave-assisted heating urea process. The obtained g-C$_3$N$_4$ exhibits enhanced H$_2$ generation rate. This strategy can be generally applicable to other nitrogen-rich precursors and capable of scale-up production of g-C$_3$N$_4$ in short time.
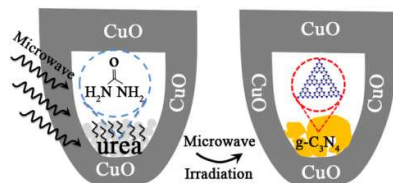
Communication

Microwave-Assisted Heating Synthesis: A General and Rapid Strategy for Large-Scale Production of High Crystalline g-C$_3$N$_4$ with Enhanced Photocatalytic H$_2$ Production

Yu-Peng Yuan,[ab] Li-Sha Yin,[b] Shao-Wen Cao,[b] Li-Na Gu,[a] Geng-Sheng Xu,[a] Pingwu Du,[*c] Hua Chai,[d] Yu-Sen Liao,[b] and Can Xue*[b]

Metal-free photocatalyst g-C$_3$N$_4$ is very attractive for solar hydrogen production. Presently, g-C$_3$N$_4$ is mainly fabricated by the conversion of nitrogen-rich precursors at high temperature (400-600 ^{o}C) for a long reaction time (several hours to multiday). Herein we report a rapid synthetic strategy named "microwave (MW)-assisted heating synthesis", which allows the high crystalline g-C$_3$N$_4$ photocatalyst to be fabricated in minutes. The obtained g-C$_3$N$_4$ displays enhanced photocatalytic H$_2$ production. In addition, the described synthetic strategy is a general approach that can also be applicable to other nitrogen-rich organic precursors, such as melamine, cyanamide, and thiourea. Importantly, the present process enables scale-up production of g-C$_3$N$_4$ for several grams in minutes.

Solar hydrogen production has been regarded as one of the most important techniques for providing renewable clean energy resources in the future. In the past decades, it has attracted tremendous efforts on developing various photocatalysts to produce hydrogen fuels through solar water splitting.[1-5] So far several UV-active and visible-response photocatalysts containing metals, such as titanium dioxide (TiO$_2$), cadmium sulfide (CdS), In$_{1-x}$Ni$_x$TaO$_4$, NaTaO$_3$, (Ga$_{1-x}$Zn$_x$)(N$_{1-x}$O$_x$), have been demonstrated as promising photocatalysts for H$_2$ production, but their limitations in terms of the requirement for UV excitation, photo-corrosion, and high cost are also noticeable.[6-10] In comparison, carbon based semiconductors become excellent candidates as new photocatalysts owing to their stability and "earth-abundant" nature.

Very recently, Wang and co-workers reported a polymeric photocatalyst, graphitic carbon nitride (g-C$_3$N$_4$), for hydrogen production using visible light.[11, 12] Unlike those metal-ion-based photocatalysts that need expensive metal salts for synthesis, the g-C$_3$N$_4$ materials can be prepared by using cheap nitrogen-rich precursors via simple polymerization process. Moreover, this metal-free photocatalyst holds high thermal and chemical stability, and has small bang gap for visible light response with suitable band edge levels for water splitting.[13-15] In addition, g-C$_3$N$_4$ has also been demonstrated for applications in carbon dioxide capture and fuel cells.[16-18] However, the synthetic methods in literatures usually require high temperature (400-600

^{o}C) with long reaction time (several hours at least) for the conversion of nitrogen-rich precursors into g-C$_3$N$_4$. For example, Wang and co-workers fabricated g-C$_3$N$_4$ materials through thermal polymerization, precipitation, and solvothermal synthesis in a period of 4~96 hours.[19-22] Thomas and co-worker reported mesoporous g-C$_3$N$_4$ through a 4 h thermal polymerization process.[23] Zou *et al* reported the thermal polymerization of melamine into g-C$_3$N$_4$ at 500 ^{o}C for 4 h.[24] All these processes are time-costly and energy-consuming. Therefore, a rapid strategy for large-scale synthesis of g-C$_3$N$_4$ becomes highly desirable for practical applications.

Herein we report a rapid synthetic strategy named "microwave (MW)-assisted heating synthesis", which allows the production of g-C$_3$N$_4$ photocatalysts in minutes through urea polymerization. The MW-assisted processes involve energy transfer from MW to the MW-absorber materials which induces strong heating in minutes, and have been widely used to fabricate various metal oxide and chalcogenide nanostructures.[25] In the present method, CuO is used as the MW-absorber that can strongly absorb MW and rapidly raise a high temperature up to 1285 K in less than 7 min at an operation power of 1 KW.[25] Interestingly, the g-C$_3$N$_4$ made by this MW-assisted process can exhibit more than 1.5 times higher photocatalytic H$_2$ generation rate than that the g-C$_3$N$_4$ produced by the thermal polymerization process (550 ^{o}C for 6 h). Importantly, this MW-assisted process is a general strategy for the g-C$_3$N$_4$ synthesis, and one can use many different nitrogen-rich small molecules as precursors, such as urea, melamine, cyanamide, and thoiurea. Moreover, this method is capable of scale-up production of g-C$_3$N$_4$ by feeding large amount of starting materials. To our knowledge, this is the first report of the MW-assisted synthesis of g-C$_3$N$_4$ photocatalysts.

Typically, the obtained products through the MW-assisted polymerization of urea are labeled as MCN$_{P-t}$, in which P refers to the MW power (W) and t is the MW heating time (min). A comparison sample of g-C$_3$N$_4$ nanosheets (Fig. S1) was also prepared by heating urea at 550 ^{o}C for 6 h in Ar (labeled as CN550) according to literature protocols (CN550 was used as the reference sample as we found that the CN550 possessed very high H$_2$ production activity in our experiments, Fig. S2).[26, 27] The model reaction, H$_2$ generation via proton reduction, was used for evaluating the photocatalytic performance of prepared g-C$_3$N$_4$

samples.

In comparison to previous synthetic methods, a distinct feature of the MW-assisted heating synthesis has very short reaction time. As shown in Fig. 1a, the sample prepared at 1000 W MW power for 18 min ($MCN_{1000-18}$) showed two distinct diffraction peaks at 13° and 27.5^o, resulting from the periodic array of the intraplanar tri-s-triazine motif stacking and the interlayer structural aromatic packing, respectively.[11] These characteristic XRD features are essentially the same as that of the CN550 sample, and indicate the formation of g-C_3N_4. However, we noted that the peak intensities of the $MCN_{1000-18}$ sample are evidently stronger than those of CN550 sample, indicating an improved crystalline quality of the $MCN_{1000-18}$ sample. This might be attributed to the MW-enhanced polymerization process that provides stronger localized heating as opposed to bulk thermal treatment. In addition, the other two weaker peaks at 18 and 22°, caused by (011) and (110) plane reflection, are also become evident when compared to those of CN550 sample.[28, 29]

The FT-IR spectrum of $MCN_{1000-18}$ is also essentially the same as that of the CN550 sample (Fig. 1b). We observed a series of bands of the typical stretching vibration modes of CN heterocycles (1640, 1568, 1460, and 1411 cm^{-1}) and the intense bending vibration mode of tri-s-triazine unit (810 cm^{-1}). The stretching vibration modes of the C-N(-C)-C and C-NH-C were also observed at 1318 and 1240 cm^{-1}, respectively. These IR bands are typical vibration modes of triazine rings. The -NH_2 stretching vibration mode appeared at around 3200 cm^{-1}. In addition, the absence of the absorption peaks at 3000 and 2200 cm^{-1} excludes the formation of the CN triple bonds.[19] All these results suggest that the polymerization of urea into g-C_3N_4 can be completed in 18 minutes. To the best of our knowledge, this case is the first example that the g-C_3N_4 photocatalyst could be synthesized within such a short time.

Typical TEM images of $MCN_{1000-18}$ sample are illustrated in Fig. 1c. The nanosheets appear as velvet-like sheets with rolling edges, as confirmed by TEM observation. The high crystalline quality of the $MCN_{1000-18}$ sample is further visualized by the HRTEM observation. Very clear HRTEM image with spacing of 0.36 nm, indexed to (002) facets, can be obtained (Fig. 1d). Comparably, the HRTEM image of CN550 is not attainable.

The band gap energy of the $MCN_{1000-18}$ sample is estimated to be 2.7 eV from the ultraviolet-visible spectrum, which is consistent with previous results (Fig. S3).[11] C/N molar ratio of $MCN_{1000-18}$ is only 0.66, deviating evidently from the theoretical ratio of 0.75 for g-C_3N_4. The elemental analysis reveals that the prepared MCN1000-18 sample is nitrogen-rich g-C_3N_4. N_2 adsorption and desorption isotherms revealed that the specific surface area (S_{BET}) of the $MCN_{1000-18}$ sample is 77 $m^2 \bullet g^{-1}$, which is higher than that of CN550 sample (65.9 $m^2 \bullet g^{-1}$). This high surface area is desirable for photocatalytic H_2 production since large surface area can provide more active sites for H_2 evolution reaction.[19]
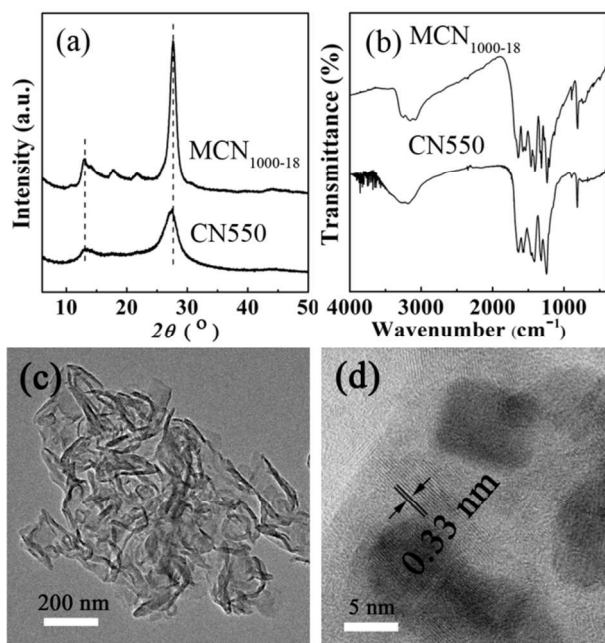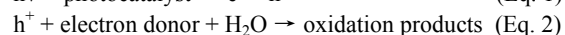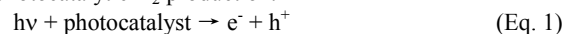

Fig. 1. Analysis of $MCN_{1000-18}$, with CN550 as reference, a) XRD patterns; b)FT-IR spectra; c) TEM image and d) HRTEM image.

Photocatalytic H_2 evolution was carried out under visible light irradiation using TEOA as the sacrificial electron donor.[30, 31] Photocatalytic reactions start from the generation of electron-hole pairs (Eq. 1), following the transfer of the photoexcited charge carriers. The added sacrificial electron donor TEOA can consume the photoexcited holes to form the oxidation products (Eq. 2) and thereby suppress the recombination of electron-hole pairs.[32] The retained electrons can then reduce water to produce hydrogen (Eq. 3).[33] All g-C_3N_4 samples were *in-situ* loaded with 0.5 wt% Pt as co-catalyst through photodeposition (Fig. S4). Control experiments showed that no H_2 evolution was detected in the absence of either photocatalysts or light irradiation. This confirmed that the hydrogen evolution requires both light irradiation and g-C_3N_4 photocatalysts. The $MCN_{1000-18}$ sample shows a H_2 evolution rate of ~ 20 $\mu mol \cdot h^{-1}$, which is more than 1.5 times higher than that of the CN550 sample (13 $\mu mol \cdot h^{-1}$) (Fig. 2a). As mentioned above, the CN550 sample possesses very high H_2 production activity.[27] When compared to the g-C_3N_4 sample obtained though melamine polymerization at $520\ ^oC$ for 2 h (labelled as M520), an enhancement over 20 times H_2 production was achieved under the same experimental conditions (~1 $\mu mol \cdot h^{-1}$, Fig. 2a). The apparent QE was determined to be 5.6 % at 420 nm by using only 10 mg g-C_3N_4 photocatalyst, which is considerably higher than literature values based on g-C_3N_4.[27] No obvious activity loss can be observed after four consecutive cycles, revealing the long-term stability of MCN1000-18 sample for photocatalytic H_2 production.

$$hv + photocatalyst \rightarrow e^- + h^+ \qquad \text{(Eq. 1)}$$
$$h^+ + electron\ donor + H_2O \rightarrow oxidation\ products \quad \text{(Eq. 2)}$$
$$e^- + H^+ \rightarrow H_2 \qquad \text{(Eq. 3)}$$

The enhanced photocatalytic H_2 production might be attributed to the enlarged surface area and the efficient separation of photogenerated electrons and holes caused by the improved crystalline quality of the $MCN_{1000-18}$ sample, as confirmed by

photocurrent measurements (Fig. 2b). The photocurrent response of the $MCN_{1000-18}$ and CN550 electrodes was measured in a 0.5 M Na_2SO_4 aqueous solution. Photocurrent generated over $MCN_{1000-18}$ is larger than that of CN550, confirming the enhanced separation of photoinduced electrons and holes in $MCN_{1000-18}$ sample. The efficient separation of photoinduced electrons and holes in $MCN_{1000-18}$ sample can further be confirmed by the ·OH radical measurement. The photoexcited holes on $MCN_{1000-18}$ sample could oxidize hydroxyl ions (OH^-) to generate ·OH radicals in the solution. It has been reported that ·OH radicals could react with terephthalic acid (TA) in basic solution to produce 2-hydroxy-terephthalic acid (TAOH), which can emit fluorescence signal with a peak centered at 426 nm.[34-36] Therefore, the TAOH fluorescence intensity can be used to quantify the ·OH radicals which are directly associated with the charge separation efficiency. As expected, the $MCN_{1000-18}$ sample shows increased TAOH fluorescence intensity in comparison to the CN550 sample. Control experiment confirms no TAOH fluorescence peak without $g-C_3N_4$ photocatalyst (Fig. 2c). The ·OH radical measurements clearly reveal that the photogenerated holes on $MCN_{1000-18}$ can generate more ·OH radicals than CN550, revealing the more effective charge separation in $MCN_{1000-18}$ than that in CN550. And this conclusion can be further verified by the enhanced photodegradation activity for methyl orange (MO) dye (Fig. S5).
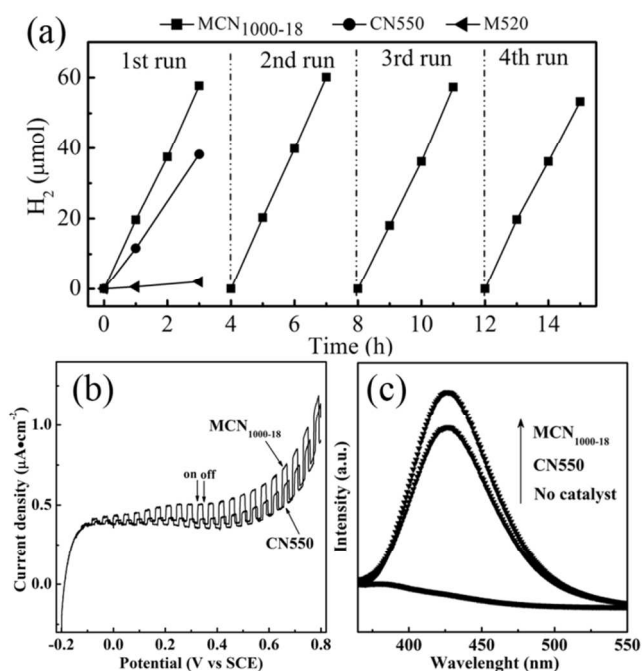

Fig. 2. (a) Photocatalytic H_2 production activity of $MCN_{1000-18}$ and CN550 sample under visible light irradiation. (b) Current-potential curves, and (c) Photoluminescence spectra of TAOH formed by the reaction of TA with ·OH radicals generated from different samples under visible light irradiation for 10 min.

We further examined the lifetime of the charge carriers in MCN1000-18 and CN550 by using time-resolved transient fluorescence spectroscopy, as shown in Fig. S6. The fitted lifetimes of the fluorescence decay profile are listed in Table S1. CN550 sample shows three radiative PL lifetime of 3.43 (weighting factor A_1=24%), 0.6 (weighting factor A_2=72%), and

17.4 ns (weighting factor A_3=4%). Comparatively, $MCN_{1000-18}$ sample also exhibits three PL lifetime components of 4.1, 0.93, and 19.55 ns, respectively. Note that the A_1 increases from 24% in CN550 to 32% in $MCN_{1000-18}$, while A_2 decreases from 72% in CN550 to 64% in $MCN_{1000-18}$. The average PL lifetime of CN550 and MCN1000-18 was 1.94 and 2.76 ns, respectively. The result evidently reveals that the longer-lived charge carriers in $MCN_{1000-18}$ allow the efficient charge separation and thus promote the photocatalytic H_2 production.

To understand the dynamics of urea polymerization under MW irradiation, we studied the urea polymerization reactions at various conditions. As shown in Fig. 3a, the characteristic XRD peaks of $g-C_3N_4$ started to show up after MW treatment of urea for 6 min (MCN_{1000-6}), indicating that the formation of $g-C_3N_4$ was initiated in very short time. However, we note that the peak corresponding to the interlayer structural aromatic systems packing rises up at 27.9° when the reaction time is less than 12 min, and moves back to its normal position at 27.5° after 15 min reaction. Further increasing the reaction time to 18 min doesn't change this peak position, but the peak intensity become stronger. Meanwhile, the in-planar reflection peak shifts significantly from 10.9° to 13.0° as the reaction time extended from 9 to 15 min. All these results demonstrate that a regular in-planar connection of the tri-s-triazine motifs in the $g-C_3N_4$ layer can form in a very short reaction time (≤ 6 min). However, some degree of the structural disorders in the tri-s-triazine connection still exists in the $g-C_3N_4$ layer when the reaction time is less than 15 min. Further extending the reaction time to 18 min led to the $g-C_3N_4$ materials with improved crystalline quality, as revealed by the enhanced XRD peak intensity. Prolonging the reaction time to 21 min causes the disappearance of the products owing to the burning out of the $g-C_3N_4$.

FT-IR spectroscopy was also used to monitor the MW-assisted urea polymerization process at different reaction time. White powders were obtained when the reaction time was less than 9 min. The FT-IR spectra clearly reveal that several bands of MCN_{1000-6} exactly agree with the bands of cyanuric acid (2781, 2449, 2109, 1779, 1722, 1398, 1053, 773, and 535 cm^{-1}), implying that urea first condenses into cyanuric acid.[37] As the reaction time increases, the intensity of these characteristic stretching bands drops, while a series of bands of the typical stretching vibration modes of CN heterocycles (1640, 1568, 1460, and 1411 cm^{-1}) and the intense bending vibration mode of tri-s-triazine unit (810 cm^{-1}) become evident (Fig. S7).[19] In particular, the intensity of C=O in cyanuric acid at 1722 cm^{-1} decreases gradually with the extended reaction time, and disappears after 12 min MW reaction. When the reaction time extends to 15 min, the shape of the spectrum is same as that of the $g-C_3N_4$, suggesting a complete conversion of urea into $g-C_3N_4$.

The structure of the intermediate products was further analyzed by ^{13}C MAS NMR (Fig. 3c). The spectrum of MCN_{1000-6} sample shows two resonance peaks at δ_1= 152.7 and δ_3= 160.5 ppm, corresponding to the C species in urea and cyanuric acid. Prolonging the reaction time to 9 min results in the disappearance of the resonance peak at δ_1= 152.7 ppm (see the spectrum of MCN_{1000-9}), indicating the total transformation of urea into cyanuric acid. The spectrum of $MCN_{1000-18}$ gives two resonance

peaks at δ_2= 156.8 and δ_4= 164.9 ppm. The first peak at δ_4= 164.9 ppm is ascribed to the C(e) atoms in $CN_2(-NH_2)$, while the second peak at δ_2= 156.8 ppm is assigned to C(i) atoms in CN_3 groups. This result is well consistent with the results previously reported by Wang et al,[20] conforming the g-C_3N_4 frameworks in $MCN_{1000-18}$. The ^{13}C MAS NMR results are in good agreement with the FT-IR results, further confirming that urea is firstly converted into cyanuric acid, and then to g-C_3N_4 (see Fig. S8).
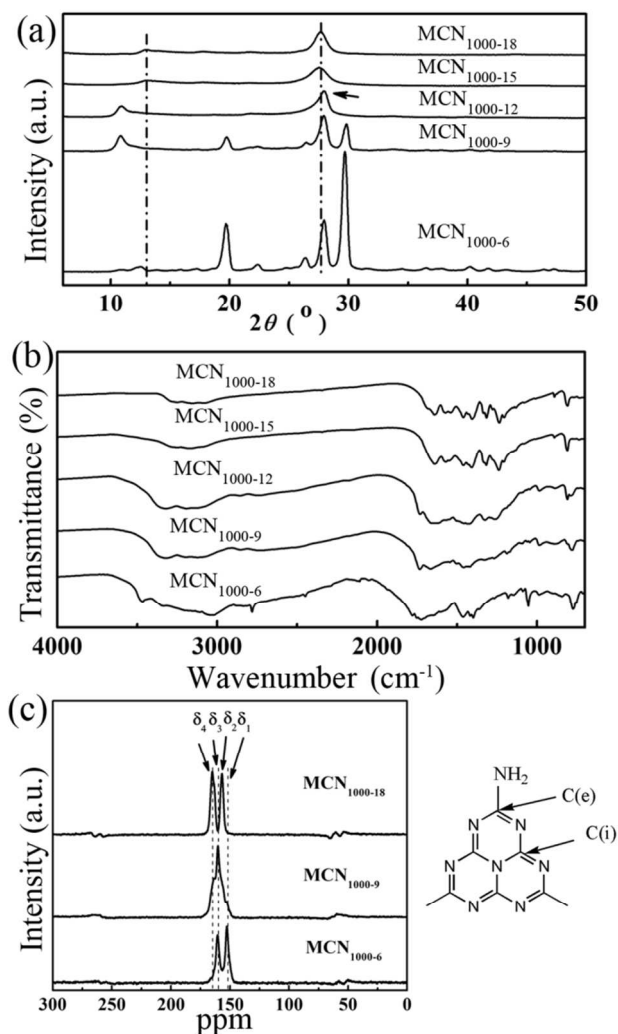
SEM observations reveal that the prolonged reaction time causes the morphology of the products from nanosheets to candy wrapper-like morphology. This candy wrapper-like morphology should be caused by the volatilization of the large volume of gas during urea decomposition (Fig. S9). N_2 adsorption and desorption isotherms revealed that S_{BET} of the obtained products greatly depends on the MW irradiation time. The S_{BET} increased from 9.7 $m^2 \bullet g^{-1}$ of MCN_{1000-9} to 56.9 $m^2 \bullet g^{-1}$ of $MCN_{1000-15}$. S_{BET} value can be further increased to 77 $m^2 \bullet g^{-1}$ for $MCN_{1000-18}$ with improved crystalline quality. This observation suggests that the extended heating time could improve the structural intactness of the g-C_3N_4, and is consistent with previous report on thermal polymerization of urea, in which larger S_{BET} of g-C_3N_4 was

observed at longer annealing time.[38] No mesopores and micropores were formed in the present g-C_3N_4 samples (Fig. S10). The optical absorption spectra were used to study the effect of the MW irradiation time on the electronic structure of g-C_3N_4 products, as shown in Fig. S11. The absorption edge of the products gradually red shifts with increased irradiation time from 9 min to 15 min. $MCN_{1000-15}$ and $MCN_{1000-18}$ samples hold the essentially same absorption edge of 460 nm, corresponding to a band gap of ~2.7 e V. These results reveal that a 15 min MW reaction time is needed to generate g-C_3N_4 with high crystalline quality to obtain reasonable photocatalytic H_2 production activity. Nevertheless, the extended MW reaction time can improve the crystalline quality, enlarge the S_{BET}, and enhance the optical absorption ability of the obtained g-C_3N_4, thus can promote the photocatalytic H_2 production (Fig. 4).

MW power also has strong impact on the polymerization reactions. At low MW output power (250 W) for 15 min, the peaks belonging to g-C_3N_4 was observed, but many intermediate species dominate in the products (Fig. S12a). Interestingly, when the reaction time prolongs to 60 min, g-C_3N_4 can also form at such a low (250 W) MW power, as revealed by the XRD pattern (Fig. S12b). In addition, we found that g-C_3N_4 can even be formed at 660 W MW power for 15 min reaction, however, some degree of disorders exists in the g-C_3N_4 layer, as revealed by the shift of the in-planar reflection peak (10.9°) (Fig. S13a). And these disorders disappear when the reaction time increases to 18 min (Fig. S13b).
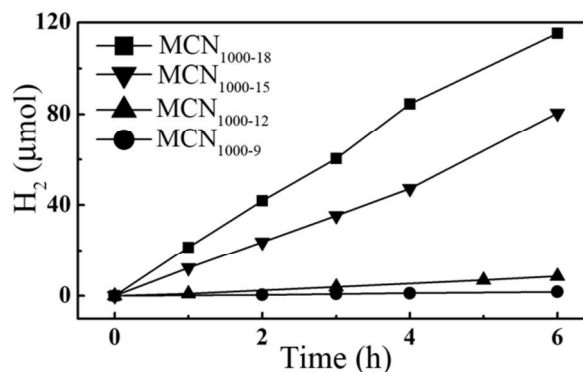

Fig. 4 Effect of MW reaction time on photocatalytic H_2 production over the obtained products.

As well known, several nitrogen-rich organic compounds containing C-N structures, such as melamine, cyanamide, thiourea, have been commonly used as starting precursors to synthesize g-C_3N_4 through thermal annealing.[21, 24, 39] In order to verify whether the present MW-assisted heating strategy can be generally applicable to these nitrogen-rich organic compounds as precursors for rapid synthesis of g-C_3N_4, we have carried out the MW-assisted synthesis by using cyanamide, melamine, and thiourea, respectively, at 1000 W MW power MW with 15-min reaction time. The XRD and FT-IR analyses (Fig. S14) confirmed that in all cases, well-crystalized g-C_3N_4 can be obtained, confirming the rapidness and generality of our strategy for g-C_3N_4 production. Moreover, all of these obtained g-C_3N_4 samples are active for photocatalytic H_2 generation under visible light irradiation (Fig. S15), though the activity is lower than that of the $MCN_{1000-15}$ sample (Fig. S16). The difference in photocatalytic H_2

production activities should be caused by the difference in particle size, morphology, crystalline quality and optical properties of the prepared g-C_3N_4 as different precursors contain various C/N ratio and chemical compositions and thereby affect the specific polymerization process. The detailed studies of the reaction time on the physical properties and photocatalytic H_2 production activities of the produced g-C_3N_4 through these nitrogen-rich small molecules will be reported later.

Most importantly, this MW-assisted synthesis can be readily scaled up for g-C_3N_4 synthesis through increasing the amount of precursors in the synthesis. For example, ~1 g of g-C_3N_4 was produced when 3 g melamine precursors was used in the synthesis. While, ~2 g of g-C_3N_4 products were obtained when the amount of the melamine precursors increased to 6 g under the same synthesis condition. Given the easy operation of our strategy, over 1 kg of g-C_3N_4 catalysts is expected to be produced through enlarging the number of the microwave over. This demonstrates that the present MW-assisted heating strategy is capable for large-scale production of g-C_3N_4 materials.

Conclusions

In summary, we have demonstrated that MW-assisted heating process is a general route for rapid and large-scale synthesis of g-C_3N_4 catalyst. This strategy holds several advantages over the conventional methods for g-C_3N_4 synthesis. First, it is a time- and energy-saving process. The reactions can be completed within several minutes. Importantly, the obtained g-C_3N_4 possesses enhanced H_2 production due to the improved crystalline quality. Second, it is a general route that can be applicable to different nitrogen-rich organic precursors. Third, this process enables scale-up production of g-C_3N_4 for several grams. Last but not the least, the MW-assisted heating process can be readily operated, and the process can be easily reproduced. We believe that this innovative strategy provides a new route to prepare g-C_3N_4 photocatalysts, and can be extended to construct doped g-C_3N_4 and hybrid materials based on g-C_3N_4 and other materials, which allows us to tailor the composition, electronic structure, and surface functionality for catalysis, energy and environmental applications.

Acknowledgements

Notes and references

[a] School of Chemistry and Chemical Engineering, Anhui University, Hefei 230039, China

[b] School of Materials Science and Engineering, Nanyang Technological University, Singapore 639798, Singapore E-mail: cxue@ntu.edu.sg (C. Xue)

[c] Department of Materials Science and Engineering, CAS Key Laboratory of Materials for Energy Conversion, University of Science and Technology of China (USTC), Hefei 230026, China Email: dupingwu@ustc.edu.cn (P. Du)

[d] School of Physical and Mathematical Sciences, Nanyang Technological University, Singapore 637371, Singapore

† Electronic Supplementary Information (ESI) available: Experimental details, SEM images; TEM images; Transient PL decay spectra; UV-visible absorption spectra; MO photodegradation; N_2 adsorption-desorption isotherms; XRD patterns; FT-IR spectra; and Photocatalytic H_2 production are included in the supporting information. See DOI:

1 A. Fujishima and K. Honda, *Nature*, 1972, **238**, 37-38.
2 A. Kudo and Y. Miseki, *Chem. Soc. Rev.*, 2009, **38**, 253-278.
3 X. B. Chen, S. H. Shen, L. J. Guo and S. S. Mao, *Chem. Rev.*, 2010, **110**, 6503-6570.
4 H. Tong, S. X. Ouyang, Y. P. Bi, N. Umezawa, M. Oshikiri and J. H. Ye, *Adv. Mater.*, 2011, **24**, 229-251.
5 Z. J. Han, F. Qiu, R. Eisenberg, P. L. Holland and T. D. Krauss, *Science*, 2012, **338**, 1321-1324.
6 G.Liu, L. Z. Wang, H. G. Yang, H. M. Cheng and G. Q. Lu, *J. Mater. Chem.*, 2010, **20**, 831-843.
7 X. Zong, H. J. Yan, G. P. Wu, G. J. Ma, F. Y. Wen, L. Wang and C. Li, *J. Am. Chem. Soc.*, 2008, **130**, 7176-7177.
8 Z. G. Zou, J. H. Ye, K. Sayama and H. Arakawa, *Nature*, **2001**, 414, 625-627.
9 H. Kato, K. Asakura and A. Kudo, *J. Am. Chem. Soc.*, **2003**, 125, 3082-3089.
10 K. Maeda, K. Teramura, D. L. Lu, T. Takata, N. Saito, Y. Inoue and K. Domen, *Nature*, 2006, **440**, 295-295.
11 X. C. Wang, K. Maeda, A. Thomas, K. Takanabe, G. Xin, J. M. Carlsson, K. Domen and M. Antonietti, *Nat. Mater.*, 2009, **8**, 76-80.
12 Y. Wang, X. C. Wang and M. Antonietti, *Angew. Chem. Int. Ed*. 2012, **51**, 68-89.
13 Y. Zheng, J. Liu, J. Liang, M. Jaroniec and S. Z. Qiao, *Energy Environ. Sci.*, 2012, **5**, 6717-6731.
14 Y. J. Zhang, A. Thomas, M. Antonietti and X. C. Wang, *J. Am. Chem. Soc.*, 2009, **131**, 50-51.
15 Y. J. Zhang, T. Mori, J. H. Ye and M. Antonietti, *J. Am. Chem. Soc.*, 2010, **132**, 6294-6295.
16 Q. A. Li, J. P. Yang, D. Feng, Z. X. Wu, Q. L. Wu, S. S. Park, C. S. Ha and D. Y. Zhao, *Nano Res*., 2010, **3**, 632-642.
17 Y. J. Zhang and M. Antonietti, *Chem. Asian J.*, 2010, **5**, 1307-1311.
18 Z. B. Zhou, R. Q. Cui, Q. J. Pang, G. M. Hadi, Z. M. Ding and W. Y. Li, *Sol. Energy Mater. Sol. Cells*, 2002, **70**, 87-92.
19 J. H. Zhang, F. S. Guo and X. C. Wang, *Adv. Funct. Mater.*, 2013, **23**, 3008-3014.
20 Y. J.Cui, Z. X. Ding, X. Z. Fu and X. C. Wang, *Angew. Chem. Int. Ed*., 2012, **51**, 11814-11818.
21 Y. S. Jun, E. Z. Lee, X. C. Wang, W. H. Hong, G. D. Stucky and A. Thomas, *Adv. Funct. Mater*., 2013, **23**, 3661-3667.
22 J. H. Sun, J. S. Zhang, M. W. Zhang, M. Antonietti, X. Z. Fu and X. C. Wang, *Nat. Comm.*, 2012, **3**, 1139.
23 Y. S. Jun, W. H. Hong, M. Antonietti and Arne Thomas, *Adv. Mater*., 2009, **21**, 4270-4274.
24 S. C. Yan, Z. S. Li and Z. G. Zou, *Langmuir*, 2010, **26**, 3894-3901.
25 K. J. Rao, B. Vaidhyanathan, M. Ganguli and P. A. Ramakrishnan, *Chem. Mater.*, 1999, **11**, 882-895.
26 Y. P. Yuan, S. W. Cao, Y. S. Liao, L. S. Yin and C. Xue *Appl. Catal. B: Environ.*, 2013, **140-141**, 164-168.
27 Y. P. Yuan, W. T. Xu, L. S. Yin, S. W. Cao, Y. S. Liao, Y. Q. Tng and C. Xue, Int. J. Hydrogen Energy, 2013, 38, 13159-13163.
28 Z. H. Zhang, K. Leinenweber, M. Bauer, L. A. J. Garvie, P. F. McMillan and G. H. Wolf, *J. Am. Chem. Soc.*, 2001, **123**, 7788-7796.
29 V D. T. odak, K. Kim, L. Iordanidis, P. G. Rasmussen, A. J. Matzger and O. M. Yaghi, *Chem. Eur. J.*, 2003, **9**, 4197-4201.
30 J. D. Hong, X. Y. Xia, Y. S. Wang and R. Xu, *J. Mater. Chem.*, 2012, **22**, 15006-15012.
31 Y. P. Yuan, S. W. Cao, L. S. Yin, L. Xu and C. Xue, *Int. J. Hydrogen Energy*, 2013, **38**, 7218-7223.
32 B. Probst, A. Rodenberg, M. Guttentag, P. Hamm and R. Alberto, *Inorg. Chem.*, 2010, **49**, 6453-6460.
33 W. Zhang, Y. B. Wang, Z. Wang, Z. Y. Zhong and R. Xu, Chem. Commun., 2010, **46**, 7631–7633.

34 T. Hirakawa and Y. Nosaka, *Langmuir*, 2002, **18**, 3247-3254.

35 J. H. Huang, K. N. Ding, X. C. Wang and X. Z. Fu, *Langmuir*, 2009, **25**, 8313-8319.

36 G. Liu, P. Niu, L. C. Yin and H. M. Cheng, *J. Am. Chem. Soc.*, 2012, **134***, 9070-9073.

37 Y. Sakata, K. Yoshimoto, K. Kawaguchi, H. Imamura and S. Higashimoto, *Catal. Today*, 2011, **161**, 41-45.

38 F. Dong, L. W. Wu, Y. J. Sun, M. Fu, Z. B. Wu and S. C. Lee, *J. Mater. Chem.*, 2011, **21**, 15171-15174.

39 F. Dong, Y. J. Sun, L. W. Wu, M. Fu and Z. B. Wu, Catal*. Sci. Technol.*, 2012, **2**, 1332-1335.

Broader context

Nowadays, the metal-free photocatalyst of graphitic carbon nitride (g-C_3N_4) is very attractive for solar hydrogen production. Presently, g-C_3N_4 was mainly fabricated by the conversion of nitrogen-rich precursors at high temperature (400-600 ^{o}C) for a long reaction time (several hours to multiday), which is time-cost and energy-consumption. Herein, we report a rapid and general synthetic strategy named "microwave (MW)-assisted heating synthesis", which allows the g-C_3N_4 photocatalysts to be fabricated in minutes. The developed synthetic strategy holds the following features. First, the present strategy is a time- and energy-efficient process. The reactions can be completed within minutes. Second, it is a general route that can be applicable to different nitrogen-rich organic precursors, such as melamine, cyanamide, and thiourea. Third, this process can enable scale-up production of g-C_3N_4 for several grams in minutes. Last but not the least, the MW-assisted heating process can be readily operated, and the process can be easily reproduced. Importantly, the obtained g-C_3N_4 possesses enhanced photocatalytic activity for H_2 production.

Green Chemistry Accepted Manuscript